

Microtubule inhibitors enhance DNA transfection efficiency through autophagy receptor p62/SQSTM1

Megumi Tsuchiya^{1#}, Hidesato Ogawa^{1#*}, Kento Watanabe¹, Takako Koujin², Chie Mori², Kazuto Nunomura³, Bangzhong Lin³, Akiyoshi Tani³, Yasushi Hiraoka^{1,2}, and Tokuko Haraguchi^{1,2*}

¹Graduate School of Frontier Biosciences, Osaka University, 1-3 Yamadaoka, Suita 565-0871, Japan

²Advanced ICT Research Institute Kobe, National Institute of Information and Communications Technology, 588-2 Iwaoka, Iwaoka-cho, Nishi-ku, Kobe 651-2492, Japan

³Graduate School of Pharmaceutical Science, Osaka University, 1-6 Yamadaoka, Suita 565-0871, Japan

These authors contributed equally to this manuscript.

*Correspondence should be addressed to:

Hidesato Ogawa, Tel: +81 668794621; Fax: +81 668794622

E-mail address: hidesato@fbs.osaka-u.ac.jp

Tokuko Haraguchi, Tel: +81 668794621; Fax: +81 668794622

E-mail address: haraguchi@fbs.osaka-u.ac.jp

Short title: Tubulin inhibitors enhance transfection efficiency

Abstract

Ectopic gene expression is an indispensable tool in biology and medicine. However, it is often limited by the low efficiency of DNA transfection. It is known that depletion of p62/SQSTM1 enhances DNA transfection efficiency by preventing the degradation of transfected DNA. Therefore, p62 is a potential target of drugs to increase transfection efficiency. To identify drugs that enhance transfection efficiency, a non-biased high-throughput screening was applied to over 4,000 compounds from the Osaka University compound library, and their p62-dependency was evaluated. The top-scoring drugs were mostly microtubule inhibitors, such as colchicine and vinblastine, and all of them showed positive effects only in the presence of p62. To understand the mechanisms, the time of p62-dependent ubiquitination was examined using polystyrene beads that were introduced into cells as materials that mimicked transfected DNA. The microtubule inhibitors caused a delay in the ubiquitination. Furthermore, the level of phosphorylated p62 at S405, which is required for ubiquitination during autophagosome formation, markedly decreased in the drug-treated cells. These results suggest that microtubule inhibitors inhibit p62-dependent autophagosome formation. Our findings provide new insights into the mechanisms of DNA transfection and also provide a solution to increase DNA transfection efficiency.

Keywords: high-throughput screening; autophagy; LC3; p62; phosphorylation; ubiquitination; gene delivery

Abbreviations: ATG, autophagy-related gene; CK2, Casein kinase 2; GAPDH, glyceraldehyde 3-phosphate dehydrogenase; GFP, green fluorescent protein; HDAC6,

48 histone deacetylase 6; KO, knockout; LC3, microtubule-associated protein light chain 3;
 49 MEF, murine embryonic fibroblast; NF- κ B, nuclear factor-kappa B; TBK1, TANK-
 50 binding kinase 1; ULK1, Unc-51 like autophagy activating kinase1; WIPI1, WD repeat
 51 domain phosphoinositide-interacting protein 1
 52

Introduction

Gene delivery is one of the most important steps for gene therapy and genetic modification in basic science. Gene therapy has great potential in clinical medicine, and this concept has become well established in therapeutic approaches. In basic science, DNA transfection is a powerful tool that enables the study of gene functions and their products in cells.

In the gene delivery process, endocytosis is a crucial pathway for the regulation of cellular uptake of plasmid DNA¹⁻³. Importantly, endocytosis can promote the induction of selective autophagy, also called xenophagy⁴. Generally, autophagy is a cytosolic bulk degradation pathway for recycling biomolecules through nonspecific degradation of proteins and organelles under nutrient starvation conditions. In contrast, selective autophagy plays an important defensive role against cellular infection by pathogens, as part of a starvation-independent autophagic defense system⁵⁻⁷. The conjugation of ubiquitin (Ub) to target pathogens is an initial and important process in selective autophagy. Ubiquitination assists in the recruitment of autophagy receptor proteins, including p62/sequestosome-1 (p62/SQSTM1), against pathogens or transfected DNA^{4, 8-11}. Therefore, suppression of the autophagy pathway can be a target for drugs to increase transfection efficiency.

We have reported that the depletion of p62/SQSTM1 protein (hereafter designated p62) greatly increases the efficiency of DNA transfection in cultured cells¹¹. To monitor the behavior of the transfected DNA, we developed an experimental system using DNA-conjugating beads that mimic the transfected DNA. In this system, DNA-conjugated beads together with pHrodo, a fluorescent marker for endosome rupture, are incorporated into cells and their intracellular dynamics are analyzed in a live cell¹¹.

Using this system, we demonstrated that the transfected DNA is incorporated into cells through endocytosis, released into the cytosol from the endosomes, and entrapped via autophagy in a p62-dependent manner. Furthermore, we demonstrated that the recruitment of Ub around the transfected material is significantly delayed in p62 gene-knockout murine embryonic fibroblast (p62KO-MEF) cells compared with that in normal MEF cells¹². Additionally, the phosphorylation of S405 (human S403) of p62 is a crucial step for the recruitment of Ub to the target site of transfected materials that mimic ectopic DNA¹¹. Hence, phosphorylation of S405 of p62 is an essential step for transfection-induced selective autophagy¹². Since p62 plays an important role in gene delivery through initial ubiquitination of the transfected DNA, inhibition of p62 may increase transfection efficiency. The aim of this study was to identify a small chemical compound that blocks the initial step of p62-dependent selective autophagy to enhance DNA transfection efficiency in mammalian cells.

Results

High-throughput screening for drugs enhancing transfection efficiency

To identify potential compounds that can enhance transfection efficiency, high-throughput screening based on a luciferase assay was performed on MEF cells using an automated workstation. MEF cells were seeded in 384-well plates and incubated for 18 h with each compound from the Osaka University compound library (4,400 compounds)¹³, at a final concentration of 10 μ M. As a negative control, DMSO (at a final concentration of 1%) was used instead of the compounds. The cells were transfected with the pCMV-Luc plasmid and incubated for 28 h; luciferase gene expression was driven by the cytomegalovirus immediate early (CMV-IE) promoter in

this plasmid. After cell viability assay, a luciferase reporter assay was carried out (Fig. 1A). Among the 4,400 compounds tested, 160 had severe effects on cell viability and were therefore removed from further analysis. For the remaining 4,240 compounds, cell viability in the presence of each compound was more than 96%. The transfection efficiency of the cells treated with each compound is plotted in Fig. 1B, the luciferase activity was normalized to cell viability. In this first screening, out of the 4,240 tested compounds, we identified 87 compounds that increased luciferase activity compared with the negative control (approximately 2.1% positive hit rate). The cutoff value used for selection was the mean value of the DMSO control + 4 × standard deviation (SD) (mean 0.347, SD = 0.242).

The activity of these 87 compounds was further analyzed via a second screening using MEF cells cultured in 96-well plates and incubated for 16 h with each of these compounds at a concentration of 1 μM. The luciferase reporter assay showed that the transfection efficiency increased in the presence of each of these compounds, with a range of approximately 2- to 260-fold that of the control, DMSO (Fig. 2A). This result indicates that all the 87 compounds exhibit a transfection-enhancing activity (Table S1). Among these, 14 were microtubule inhibitors. Notably, the top 10 compounds were all microtubule inhibitors, including colchicine and vinblastine (Fig. 2B).

Microtubule inhibitors enhance gene transfection efficiency

To further evaluate the effects of these compounds on DNA transfection efficiency, we selected two well-used microtubule inhibitors: colchicine and vinblastine. These were ranked second and third, respectively, in the 2nd screening (Fig. 2A). Firstly, we

examined the dose-dependency of these inhibitors in MEF cells (Fig. 2C). Cells were treated with colchicine or vinblastine at various concentrations, and transfected with the pCMV-Luc DNA plasmid. The luciferase activity was then measured. The transfection efficiency increased in a chemical dose-dependent manner in the MEF cells (Fig. 2C). Statistical analysis showed that the EC₅₀ of colchicine and vinblastine was 239.1 and 26.29 nM, respectively, in the MEF cells (Fig. 2C). Furthermore, we evaluated the transfection efficiency by measuring the fluorescence level of the GFP expressed in the MEF cells. There were greater numbers of GFP-positive cells among the MEF cells treated with colchicine or vinblastine than among the DMSO-treated control cells (Fig. 2D). These results suggest that treatment with colchicine and vinblastine can enhance transfection efficiency.

It has been reported that depolymerization of microtubules activates the transcription factor, NF- κ B, and induces NF- κ B-dependent gene expression¹⁴. Therefore, it is possible that treatment with microtubule inhibitors may induce the activation of gene expression through NF- κ B activation. In fact, the CMV promoter, which is used in the pCMV-Luc plasmid, possesses an NF- κ B binding site^{14, 15}; therefore, this can affect luciferase gene expression via promoter activation. To test this possibility, we established a cell line (MEF-LUC cells) with a CMV-driven luciferase plasmid integrated into the genome. These cells were treated with colchicine or vinblastine for 16 h, and the levels of luciferase activity were measured in the presence and absence of colchicine or vinblastine (Fig. S1). Treatment with colchicine showed only a slight increase in luciferase gene expression, and its fold-increase was much lower than that of DNA transfection (Fig. S1; compare with Fig. 2C). Treatment with vinblastine also showed a similar result, with almost no increase in luciferase

expression. These results suggest that colchicine and vinblastine affect transfection efficiency, but not by enhancing promoter activity.

Transfection enhancement occurs in the presence of autophagy receptor p62

Since p62 acts as an inhibitory factor for DNA transfection¹¹, the transfection-enhancing activity of tested compounds may be deduced by the invalidation of the p62-dependent autophagic pathway. Based on this hypothesis, we examined the activity of the 87 compounds at a concentration of 1 μ M in p62KO-MEF cells under the same condition as in Fig. 2A (Fig. 3A). All of them exhibited no or little transfection-enhancing activity in p62KO-MEF cells (Fig. 3A). As microtubule inhibitors (compounds 1-10 in Figs. 2A, 2B and 3A) seemed to show slight increase of transfection enhancing activity, we further tested colchicine and vinblastine for transfection-enhancing activity at various concentrations from 15.6 to 2000 nM (Figs. 3B and 3C), and found that these two microtubule inhibitors did not show transfection-enhancing activity at any of the concentrations tested in those cells (Fig. 3B and 3C). This result suggests that microtubule inhibitors function in a p62-dependent autophagic pathway. This is consistent with the recruitment of microtubule-associated protein 1A/1B-light chain 3 (LC3; also called ATG8), a marker protein for autophagosome, to transfected DNA, which occurs in a p62-dependent manner¹¹.

p62-dependent ubiquitination is delayed by microtubule inhibitors

To understand the molecular mechanisms of the p62-dependent enhancement of transfection efficiency by colchicine and vinblastine, we employed an experimental method using polystyrene beads that had been developed to monitor the behavior of the

transfected DNA¹⁶ (Fig. 4A). In this method, the beads are incorporated into cells with transfection reagents via endocytosis and enter the cytosol after rupture of the endosomal membrane. The beads that appeared in the cytosol were targeted for autophagy, similar to the transfected DNA^{16, 17} (Fig. 4A). To monitor them in living cells, the beads were pre-conjugated with pHrodo dye, which emits fluorescence under acidic pH conditions, such as in the acidic endosome, but not in the cytosol. This dye, therefore, serves as a marker of endosome membrane rupture, as described previously¹⁶. The pHrodo-conjugated beads were incorporated into MEF cells expressing a GFP-fused Ub protein (GFP-Ub MEF cells)¹², and the assembly of GFP-Ub around the beads was observed in a living cell using time-lapse fluorescence microscopy (Fig. 4B). In the control DMSO-treated cells, the time for Ub recruitment to the beads was approximately 3–4 min (Fig. 4B, middle panel) after pHrodo fluorescence disappeared (Fig. 4B, upper panel). In contrast, the time for GFP-signal accumulation was 9–10 min in 500 nM colchicine-treated MEF cells (Fig. 4C, middle panel), which was longer than that in the control cells (Fig. 4B). Statistical analysis was performed to determine the timing of GFP-signal accumulation around the beads after the loss of pHrodo signals in cells expressing GFP-Ub with or without the inhibitor (Fig. 4D). It showed that, in the DMSO-treated cells, the time for Ub recruitment to the beads was ~4 min (median) after pHrodo fluorescence disappeared (mean and SD, 4.167 ± 1.88 min, $n = 24$ beads; lane 1 in Fig. 4D). Moreover, the timing of GFP-signal accumulation was ~6 min (median) in 100 nM colchicine-treated MEF cells (mean and SD: 8.286 ± 8.36 min, $n = 28$ beads: lane 2 in Fig. 4D), ~11 min (median) in 500 nM colchicine-treated MEF cells (mean and SD: 11.32 ± 11.30 min, $n = 22$ beads: lane 3 in Fig. 4D), and ~6 min (median) in the vinblastine-treated MEF cells (mean and SD: 6.48 ± 3.81 min, $n = 31$ beads; lane 4

in Fig. 4D). Additionally, the GFP-Ub signals did not accumulate within 60 min in colchicine- or vinblastine-treated GFP-Ub MEF cells (these beads were not counted and were not included in the n ; upper coloum in Fig. 4D). These results show that GFP-Ub accumulation to the beads is significantly delayed in the colchicine- or vinblastine-treated MEF cells, and also suggest that intact microtubules are important for the recruitment of Ub to the target sites.

The active form of p62 is suppressed by microtubule inhibitors

It has been reported that the phosphorylated form of p62 at the amino acid residue S405 (p62 S405) is required for Ub recruitment in the process of selective autophagy¹². Therefore, Ub recruitment can be delayed by a decrease in the level of phosphorylated p62 at S405. To test this idea, we performed Western blot analysis to evaluate total p62 protein levels and p62 S405 phosphorylation levels (Fig. 5). Before DNA transfection (0 h), the p62 S405 phosphorylation levels were very low. However, after transfection (24 h), these levels greatly increased in DMSO-treated MEF cells, although the p62 levels remained unchanged. This suggests that DNA transfection induces an increase in p62 S405 phosphorylation. In the MEF cells treated with colchicine or vinblastine, however, the levels of p62 S405 phosphorylation decreased. This suggests that microtubule inhibitors inhibit Ub recruitment by decreasing the level of phosphorylated p62 S405, which is required for Ub recruitment in selective autophagy. This implies that microtubule inhibitors are responsible for the delay in Ub recruitment and therefore increase transfection efficiency in MEF cells.

Discussion

Microtubule structure/function and transfection efficiency

In this study, we used a non-biased, high-throughput screening approach to identify small chemical compounds that increase DNA transfection efficiency. The top 10 compounds were all microtubule inhibitors. Therefore, inhibition of the microtubule structure or function seems to trigger an increase in transfection efficiency. This finding is consistent with previous reports on cultured vascular smooth muscle cells and CV-1 cells, in which microtubule inhibitors, such as colchicine, vinblastine, vincristine, nocodazole, and podophyllotoxin, increased the transfection efficiency^{15, 18}. Interestingly, some reports showed that microtubule-polymerizing agents, such as paclitaxel, also increased the transfection efficiency in COS-7 and A549 cells^{19, 20}. The polymerizing agent, docetaxel, a chemical compound closely related to paclitaxel, was included in our screening results for the top 10 compounds (Fig. 2B, Rank 7). Moreover, tubulin deacetylation inhibitors, such as HDAC6 inhibitors, also increased the transfection efficiency in A549 cells, TC7 cells, and mesenchymal stem cells²¹⁻²³. This is likely because acetylated tubulin can stabilize microtubule structures, which in turn implies that microtubule structure stabilization can also increase gene transfection efficiency. Taken together, these findings strongly suggest that inhibition of the intact structure or dynamic nature of microtubules is important for increasing the efficiency of gene transfection.

Microtubule inhibitors affect selective autophagy pathways

Our results showed that treatment of cells with colchicine or vinblastine increased transfection efficiency in a p62-dependent manner. However, it is difficult to attribute these observations to one particular cause. Since microtubules are major contributors to

the trafficking of several components in the endosomal/lysosomal pathway, it is logical to propose that these inhibitors may block the autophagy pathway. The role of microtubules in autophagosome formation appears to be different based on the culture medium conditions, e.g., vegetatively growing medium (basal) or starvation medium (inducible) conditions. Several studies have used microtubule inhibitors under basal conditions to show that microtubules do not participate in autophagosome formation²⁴⁻²⁶. However, under inducible conditions, disassembling the microtubules with these inhibitors prevented autophagosome formation, suggesting that the role of microtubules is crucial in this step^{25, 27}. Previous studies have shown that transfected DNA also induces the selective autophagy pathway^{4, 9, 11}; hence, microtubule inhibitors may affect transfection-induced autophagosome formation. The detailed mechanisms of the inhibition of autophagosome formation following microtubule inhibitor treatment are not clear; however, several autophagy factors are associated with microtubules, including ATG8 (LC3), ATG1 (ULK1), ATG6 (Beclin1), ATG18 (WIP1), and p62²⁸. LC3 has long been thought to be involved in the regulation of the assembly and disassembly of microtubules^{29, 30}. Furthermore, ATG18-positive pre-autophagosomal structures can move along microtubules, and this movement is highly sensitive to microtubule inhibitor treatment³¹. These data suggest that microtubules contribute to the sequestration, recruitment, and movement of autophagy factors for the formation of the inducible autophagosome. Therefore, microtubule inhibitors may block the inducible autophagy pathway, resulting in a decrease in the likelihood of DNA degradation and an increase in the transfection efficiency.

Microtubule inhibitors decrease the level of phosphorylated p62

The ubiquitination of endosome membrane proteins surrounding exogenous material, such as transfected DNA, is the initial step in inducible selective autophagy^{11, 32, 33}. In our study, treatment with colchicine or vinblastine delayed the recruitment of Ub proteins. This delay in recruitment is also caused by depletion of p62 or the mutation of the phosphorylation site at S405 of p62 (human S403)¹². Since p62 has been reported as one of the microtubule-associated factors²⁷, treatment with a microtubule inhibitor may affect p62-mediated Ub recruitment. Specifically, our results showed that p62 S405 phosphorylation was significantly impaired by treatment with colchicine or vinblastine after transfection. p62 S405 is phosphorylated by kinases such as CK2 and TBK1^{34, 35}. These kinases are also associated with tubulin³⁶⁻³⁹. After transfection, the recruitment of these kinases may be affected by treatment with microtubule inhibitors. Further studies are necessary to elucidate the detailed mechanisms by which these microtubule inhibitors can affect the phosphorylation levels of p62.

In this study, a non-biased high-throughput screening method demonstrated that microtubule inhibitors enhanced transfection efficiency in a p62-dependent manner. This indicates that p62 function is associated with microtubule structure, and this function is critical for the control of transfection efficiency.

Materials and Methods

Plasmids

The pGL4.50 [*luc2*/CMV/Hygro] vector (NCBI Accession: EU921840.1), which encodes the luciferase reporter gene *luc2*, was used as a luciferase expression vector and named pCMV-Luc (E1310; Promega, Madison, WI, USA). The GFP expression

plasmid pCMX-AFAP was prepared as previously described⁴⁰. pBABE-puro was purchased from Addgene (1764; Addgene, Cambridge, MA, USA).

To create the PB-CMV-LUC-Zeo vector, we first constructed the PB-EF1-MCS-IRES-Zeo vector. To insert the zeocin resistance gene DNA sequence, two DNA fragments (#1 and #2) were amplified as follows: the cloning site with Kozak sequence fragment #1 was amplified from the PB-EF1-MCS-IRES-Neo vector (PB533A-2; System Biosciences, Palo Alto, CA, USA) using PCR and the following primers: 5'-CTGAAGGATGCCCAGAAGGTACCCCATTGT-3' and 5'-TCCGGACGCCATGGTTGTGG-3'. The zeocin cord fragment #2 was amplified from the pcDNA3.1/Zeo(+) vector (V86020; Thermo Fisher Scientific, Yokohama, Japan) using PCR and the following primers: 5'-ACAACCATGGCGTCCGGAATGGCCAAGTTGACCAGTGCCGTTCC-3' and 5'-TCCAGAGGTTGATTGTCGACTCAGTCCTGCTCCTCGGCCACGAA-3'. Following digestion with KpnI and SalI, fragments #1 and #2 were inserted into the PB-EF1-MCS-IRES-Neo vector using the In-Fusion HD Cloning Kit (639648; Takara Bio Inc. Kusatsu, Japan.). This resulted in the PB-EF1-MCS-IRES-Zeo vector.

Next, the human cytomegalovirus immediate early enhancer and promoter (CMV-IE) DNA sequence (#3) was amplified from the pGL4.50 [*luc2*/CMV/Hygro] vector using PCR and the following primers: 5'-GGGGATACGGGGAAAAGGCCTCGTTACATAACTTACGGTAAATG-3' and 5'-GAATTCGCTAGCTCTAGAAGCTCTGCTTATATAGACCTCCCACC-3'. The luciferase DNA sequence (#4) was amplified from the pGL4.50 [*luc2*/CMV/Hygro] vector using PCR and the following primers: 5'-TCTAGAGCTAGCGAATTCATGGAAGATGCCAAAACATTAAGAA-3'

and 5'-CGATTTAAATTCGAATTCTTACACGGCGATCTTGCCGCCCTTCT-3'.

Following digestion with EcoRI and StuI, fragments #3 and #4 were inserted into the PB-EF1-MCS-IRES-Zeo vector using the In-Fusion HD Cloning Kit. This resulted in the PB-CMV-LUC-Zeo vector.

Cell Strains

p62KO-MEF cells (p62^{-/-} cells) and their parental MEF cells were kindly provided by Dr. Tetsuro Ishii (University of Tsukuba)⁴¹. MEF cells stably expressing GFP-Ub were generated as previously described¹². Briefly, to obtain MEF cells or p62KO-MEF cells stably expressing luciferase, MEF cells or p62KO-MEF cells were transfected with the PB-CMV-LUC-Zeo plasmid and cultured in the presence of 100 µg/mL Zeocin (R25501, Thermo Fisher Scientific), and then single clones (MEF-LUC cells) were selected. Each stable clone was examined for luciferase protein expression using a luciferase reporter gene assay.

Cell Culture

All cell lines were maintained in Dulbecco's Modified Eagle Medium (DMEM) (D6429; Sigma-Aldrich, St. Louis, MO, USA) supplemented with 10% fetal bovine serum in the presence of 5% CO₂ at 37°C.

High-Throughput Screening for enhancer compounds

MEF cells were seeded at a density of 0.8×10^3 cells per well (384-well microplate, 781091; Greiner Bio-One, Tokyo, Japan) using a Multidrop COMBI (Thermo Fisher Scientific), and incubated in culture medium for 6 h. The cells were treated with 1%

DMSO (negative control) or the screening compounds (10 μ M each) using Fluent780® Automation Workstation (Tecan Japan, Kawasaki, Japan) with a 96-channel head adapter and Tecan sterile tips (30048824; Tecan Japan). After 16 h, the cells were transfected with 25 ng of pCMV-Luc plasmid using Lipofectamine 2000 (Thermo Fisher Scientific) according to the manufacturer's protocol. The cells were then incubated for 28 h, followed by measurement of cell viability with the RealTime-Glo™ MT Cell Viability Assay (E9713; Promega) using the GloMax® Discover Microplate Reader (Promega). Luciferase activity was measured with the ONE-Glo™ Luciferase Assay System (E6120; Promega) using the GloMax® Discover Microplate Reader.

Luciferase Assays

Cells were seeded at a density of 0.45×10^4 cells per well (96-Well Assay Plate; 3603 Corning, Corning, NY, USA) and incubated in culture medium for 6 h. The cells were treated with 1% DMSO (negative control) or the screening compounds (0.1–10 μ M each). After 16 h, the cells were transfected with 100 ng of pCMV-Luc plasmid using Lipofectamine 2000 according to the manufacturer's protocol. The cells were then incubated for 28 h, followed by measurement of cell viability with the RealTime-Glo™ MT Cell Viability Assay to normalize cell number using the GloMax™ 96 Microplate Luminometer (Promega). Luciferase activity was measured with the ONE-Glo™ Luciferase Assay System using the GloMax™ 96 Microplate Luminometer. The mean EC50 values and standard deviations were determined from three independent experiments.

Preparation of pHrodo-conjugated Beads

pHrodo-conjugated beads were prepared as previously described¹⁶. Briefly, Dynabeads M-270 Streptavidin (DB65306; Thermo Fisher Scientific) were washed three times with phosphate buffered saline (PBS) and resuspended in 100 mM sodium bicarbonate buffer (pH 8.5) to an appropriate concentration (typically a 1:10 or 1:20 dilution). pHrodo-succinimidyl ester (P36600; Thermo Fisher Scientific) was then added to the bead suspension and incubated in sodium bicarbonate buffer for 1 h at room temperature (about 26°C). After the conjugation reaction, the beads were washed with sodium bicarbonate buffer and suspended in PBS.

Incorporation of Beads into Living Cells

Beads were incorporated into cells as previously described¹⁷. One day before incorporating the beads, GFP-Ub MEF cells were seeded onto 35-mm glass-bottom culture dishes (P35G-1.5-10-C; MatTek, Ashland, MA, USA) at a density of 1.5×10^5 cells/dish in culture medium. Transfection-reagent-coated beads were prepared by mixing pHrodo-conjugated beads with Effectene transfection reagent (301425; Qiagen, Tokyo, Japan) according to the manufacturer instructions, except that the bead suspension was used instead of DNA solution. The resulting bead mixture (~10 µL) was mixed with 90 µL of the culture medium and added to the cells by replacing the medium. After incubation for 1 h at 37°C in a CO₂ incubator, the cells were washed twice with fresh growth medium to remove unattached beads and then further incubated for the time indicated in each experiment.

Time-Lapse Imaging

Cells were treated with 100 ng/mL Hoechst33342 (B2261; Sigma-Aldrich) for 15 min to stain chromosomes, as previously described⁴². After replacing the culture medium with fresh medium not containing phenol red, time-lapse observation was performed using an oil-immersion objective lens (UApo40/NA1.35; Olympus, Tokyo, Japan) on a DeltaVision microscope system (GE Healthcare Life Sciences Japan, Tokyo, Japan) placed in a temperature-controlled room (37°C), as previously described⁴². Images were obtained every minute for ~60 min.

Western Blot Analysis

Western blot analysis was performed as previously described¹². Briefly, cell lysates were prepared in a lysis buffer [50 mM Tris-HCl, pH 7.5, 150 mM NaCl, 1 mM EDTA, 1% Triton X-100, 1 x Phosphatase Inhibitor Cocktail Solution II (160-24371; FUJIFILM Wako Pure Chemical Corporation, Osaka, Japan) and 1 x protease inhibitor cocktail (Nacalai tesque Inc., Kyoto, Japan)]. The lysates were subjected to electrophoresis on NuPAGE 4% to 12% Bis-Tris gels (NP0321; Thermo Fisher Scientific). Proteins were transferred to polyvinylidene fluoride membranes and probed using anti-p62(SQSTM1) (PM045; MBL, Nagoya, Japan), anti-Phospho-SQSTM1/p62(Ser403) (D8D6T; Cell Signaling Technology, Danvers, MA, USA), and anti-glyceraldehyde 3-phosphate dehydrogenase (GAPDH) (14C10; Cell Signaling Technology) antibodies, and secondary antibody conjugated to horseradish peroxidase (NA9340V; GE Healthcare Life Sciences). Protein bands were stained with ImmunoStar Zeta (295-72404; FUJIFILM Wako Pure Chemical Corporation) and detected by chemiluminescence using a ChemiDoc MP imaging system (Bio-Rad, Tokyo, Japan).

411

412 *Statistical Analysis*

413 The *p*-values were obtained by performing Kruskal-Wallis tests using GraphPad Prism
414 8 software (GraphPad Software, Inc., La Jolla, CA, USA).

415

416 *Acknowledgments*

417 We are grateful to Dr. Eiji Warabi and Dr. Tetsuro Ishii (Tsukuba University) for
418 providing p62KO-MEF cells and the corresponding wild-type MEF cells. We thank J.
419 Iacona, Ph.D., from Edanz Group (<https://en-author-services.edanzgroup.com/ac>) for
420 English-editing a draft of this manuscript. This study was supported by The JSPS
421 Kakenhi Grant Numbers JP19K06488 to MT, JP19KK0218, JP20H05322 and
422 JP20K07029 to HO, JP18H05533 to YH, and JP17K19505 and JP18H05528 to TH.
423 This research was supported by Platform Project for Supporting Drug Discovery and
424 Life Science Research (Basis for Supporting Innovative Drug Discovery and Life
425 Science Research (BINDS)) from AMED under Grant Number JP20am0101084.

426

427 *Author contributions*

428 MT, HO, KW, TK, CM, KN, BL and AT performed the experiments. MT, HO, AT,
429 YH, and TH designed the experiments. All authors analyzed and discussed the data, and
430 MT, HO, YH, and TH wrote the manuscript.

431

432 *Conflict of Interest*

433 All authors declare that: (i) no support, financial or otherwise, has been received from
434 any organization that may have an interest in the submitted work; and (ii) there are no
435 other relationships or activities that could appear to have influenced the submitted work.
436

Reference

1. Khalil, IA, Kogure, K, Akita, H, and Harashima, H (2006). Uptake pathways and subsequent intracellular trafficking in nonviral gene delivery. *Pharmacol Rev* **58**: 32-45.
2. Midoux, P, Breuzard, G, Gomez, JP, and Pichon, C (2008). Polymer-based gene delivery: a current review on the uptake and intracellular trafficking of polyplexes. *Curr Gene Ther* **8**: 335-352.
3. Rejman, J, Bragonzi, A, and Conese, M (2005). Role of clathrin- and caveolae-mediated endocytosis in gene transfer mediated by lipo- and polyplexes. *Mol Ther* **12**: 468-474.
4. Chen, X, Khambu, B, Zhang, H, Gao, W, Li, M, Chen, X, *et al.* (2014). Autophagy induced by calcium phosphate precipitates targets damaged endosomes. *J Biol Chem* **289**: 11162-11174.
5. Nakatogawa, H, Suzuki, K, Kamada, Y, and Ohsumi, Y (2009). Dynamics and diversity in autophagy mechanisms: lessons from yeast. *Nature reviews Molecular cell biology* **10**: 458-467.
6. Mizushima, N, Yoshimori, T, and Ohsumi, Y (2011). The role of Atg proteins in autophagosome formation. *Annu Rev Cell Dev Biol* **27**: 107-132.
7. Galluzzi, L, Baehrecke, EH, Ballabio, A, Boya, P, Bravo-San Pedro, JM, Cecconi, F, *et al.* (2017). Molecular definitions of autophagy and related processes. *The EMBO journal* **36**: 1811-1836.
8. Dupont, N, Temime-Smaali, N, and Lafont, F (2010). How ubiquitination and autophagy participate in the regulation of the cell response to bacterial infection. *Biology of the cell* **102**: 621-634.

- 461 9. Roberts, R, Al-Jamal, WT, Whelband, M, Thomas, P, Jefferson, M, van den
462 Bossche, J, *et al.* (2013). Autophagy and formation of tubulovesicular
463 autophagosomes provide a barrier against nonviral gene delivery. *Autophagy* **9**:
464 667-682.
- 465 10. Alomairi, J, Bonacci, T, Ghigo, E, and Soubeyran, P (2015). Alterations of host
466 cell ubiquitination machinery by pathogenic bacteria. *Frontiers in cellular and*
467 *infection microbiology* **5**: 17.
- 468 11. Tsuchiya, M, Ogawa, H, Koujin, T, Kobayashi, S, Mori, C, Hiraoka, Y, *et al.*
469 (2016). Depletion of autophagy receptor p62/SQSTM1 enhances the efficiency
470 of gene delivery in mammalian cells. *FEBS letters* **590**: 2671-2680.
- 471 12. Tsuchiya, M, Ogawa, H, Koujin, T, Mori, C, Osakada, H, Kobayashi, S, *et al.*
472 (2018). p62/SQSTM1 promotes rapid ubiquitin conjugation to target proteins
473 after endosome rupture during xenophagy. *FEBS Open Bio* **8**: 470-480.
- 474 13. Tachibana, K, Yuzuriha, T, Tabata, R, Fukuda, S, Maegawa, T, Takahashi, R, *et*
475 *al.* (2018). Discovery of peroxisome proliferator-activated receptor alpha
476 (PPARalpha) activators with a ligand-screening system using a human
477 PPARalpha-expressing cell line. *J Biol Chem* **293**: 10333-10343.
- 478 14. Rosette, C, and Karin, M (1995). Cytoskeletal control of gene expression:
479 depolymerization of microtubules activates NF-kappa B. *The Journal of cell*
480 *biology* **128**: 1111-1119.
- 481 15. Wang, L, and MacDonald, RC (2004). Effects of microtubule-depolymerizing
482 agents on the transfection of cultured vascular smooth muscle cells: enhanced
483 expression with free drug and especially with drug-gene lipoplexes. *Mol Ther* **9**:
484 729-737.

- 485 16. Kobayashi, S, Kojidani, T, Osakada, H, Yamamoto, A, Yoshimori, T, Hiraoka, Y,
486 *et al.* (2010). Artificial induction of autophagy around polystyrene beads in
487 nonphagocytic cells. *Autophagy* **6**: 36-45.
- 488 17. Kobayashi, S, Koujin, T, Kojidani, T, Osakada, H, Mori, C, Hiraoka, Y, *et al.*
489 (2015). BAF is a cytosolic DNA sensor that leads to exogenous DNA avoiding
490 autophagy. *Proceedings of the National Academy of Sciences of the United*
491 *States of America* **112**: 7027-7032.
- 492 18. Lindberg, J, Fernandez, MA, Ropp, JD, and Hamm-Alvarez, SF (2001).
493 Nocodazole treatment of CV-1 cells enhances nuclear/perinuclear accumulation
494 of lipid-DNA complexes and increases gene expression. *Pharmaceutical*
495 *research* **18**: 246-249.
- 496 19. Hasegawa, S, Hirashima, N, and Nakanishi, M (2001). Microtubule involvement
497 in the intracellular dynamics for gene transfection mediated by cationic
498 liposomes. *Gene Ther* **8**: 1669-1673.
- 499 20. Nair, RR, Rodgers, JR, and Schwarz, LA (2002). Enhancement of transgene
500 expression by combining glucocorticoids and anti-mitotic agents during
501 transient transfection using DNA-cationic liposomes. *Mol Ther* **5**: 455-462.
- 502 21. Barua, S, and Rege, K (2010). The influence of mediators of intracellular
503 trafficking on transgene expression efficacy of polymer-plasmid DNA
504 complexes. *Biomaterials* **31**: 5894-5902.
- 505 22. Ho, YK, Zhou, LH, Tam, KC, and Too, HP (2017). Enhanced non-viral gene
506 delivery by coordinated endosomal release and inhibition of beta-tubulin
507 deacetylase. *Nucleic acids research* **45**: e38.
- 508 23. Vaughan, EE, Geiger, RC, Miller, AM, Loh-Marley, PL, Suzuki, T, Miyata, N, *et*

509 *al.* (2008). Microtubule acetylation through HDAC6 inhibition results in
510 increased transfection efficiency. *Mol Ther* **16**: 1841-1847.

511 24. Aplin, A, Jasionowski, T, Tuttle, DL, Lenk, SE, and Dunn, WA, Jr. (1992).
512 Cytoskeletal elements are required for the formation and maturation of
513 autophagic vacuoles. *J Cell Physiol* **152**: 458-466.

514 25. Kochl, R, Hu, XW, Chan, EY, and Tooze, SA (2006). Microtubules facilitate
515 autophagosome formation and fusion of autophagosomes with endosomes.
516 *Traffic (Copenhagen, Denmark)* **7**: 129-145.

517 26. Reunanen, H, Marttinen, M, and Hirsimäki, P (1988). Effects of griseofulvin and
518 nocodazole on the accumulation of autophagic vacuoles in Ehrlich ascites tumor
519 cells. *Exp Mol Pathol* **48**: 97-102.

520 27. Geeraert, C, Ratier, A, Pfisterer, SG, Perdiz, D, Cantaloube, I, Rouault, A, *et al.*
521 (2010). Starvation-induced hyperacetylation of tubulin is required for the
522 stimulation of autophagy by nutrient deprivation. *J Biol Chem* **285**: 24184-
523 24194.

524 28. Mackeh, R, Perdiz, D, Lorin, S, Codogno, P, and Pous, C (2013). Autophagy and
525 microtubules - new story, old players. *Journal of cell science* **126**: 1071-1080.

526 29. Mann, SS, and Hammarback, JA (1994). Molecular characterization of light
527 chain 3. A microtubule binding subunit of MAP1A and MAP1B. *J Biol Chem*
528 **269**: 11492-11497.

529 30. Deretic, V (2008). Autophagosome and phagosome. *Methods Mol Biol* **445**: 1-
530 10.

531 31. Polson, HE, de Lartigue, J, Rigden, DJ, Reedijk, M, Urbe, S, Clague, MJ, *et al.*
532 (2010). Mammalian Atg18 (WIPI2) localizes to omegasome-anchored

533 phagophores and positively regulates LC3 lipidation. *Autophagy* **6**: 506-522.

534 32. Randow, F (2011). How cells deploy ubiquitin and autophagy to defend their
535 cytosol from bacterial invasion. *Autophagy* **7**: 304-309.

536 33. Wileman, T (2013). Autophagy as a defence against intracellular pathogens.
537 *Essays in biochemistry* **55**: 153-163.

538 34. Matsumoto, G, Shimogori, T, Hattori, N, and Nukina, N (2015). TBK1 controls
539 autophagosomal engulfment of polyubiquitinated mitochondria through
540 p62/SQSTM1 phosphorylation. *Human molecular genetics* **24**: 4429-4442.

541 35. Matsumoto, G, Wada, K, Okuno, M, Kurosawa, M, and Nukina, N (2011).
542 Serine 403 phosphorylation of p62/SQSTM1 regulates selective autophagic
543 clearance of ubiquitinated proteins. *Molecular cell* **44**: 279-289.

544 36. Faust, M, Schuster, N, and Montenarh, M (1999). Specific binding of protein
545 kinase CK2 catalytic subunits to tubulin. *FEBS letters* **462**: 51-56.

546 37. Lim, AC, Tiu, SY, Li, Q, and Qi, RZ (2004). Direct regulation of microtubule
547 dynamics by protein kinase CK2. *J Biol Chem* **279**: 4433-4439.

548 38. Pillai, S, Nguyen, J, Johnson, J, Haura, E, Coppola, D, and Chellappan, S
549 (2015). Tank binding kinase 1 is a centrosome-associated kinase necessary for
550 microtubule dynamics and mitosis. *Nature communications* **6**: 10072.

551 39. Yang, H, Mao, W, Rodriguez-Aguayo, C, Mangala, LS, Bartholomeusz, G, Iles,
552 LR, *et al.* (2018). Paclitaxel Sensitivity of Ovarian Cancer Can be Enhanced by
553 Knocking Down Pairs of Kinases that Regulate MAP4 Phosphorylation and
554 Microtubule Stability. *Clin Cancer Res* **24**: 5072-5084.

555 40. Ogawa, H, Yu, RT, Haraguchi, T, Hiraoka, Y, Nakatani, Y, Morohashi, K, *et al.*
556 (2004). Nuclear structure-associated TIF2 recruits glucocorticoid receptor and

557 its target DNA. *Biochemical and biophysical research communications* **320**:
558 218-225.

559 41. Komatsu, M, Waguri, S, Koike, M, Sou, YS, Ueno, T, Hara, T, *et al.* (2007).
560 Homeostatic levels of p62 control cytoplasmic inclusion body formation in
561 autophagy-deficient mice. *Cell* **131**: 1149-1163.

562 42. Haraguchi, T, Kaneda, T, and Hiraoka, Y (1997). Dynamics of chromosomes and
563 microtubules visualized by multiple-wavelength fluorescence imaging in living
564 mammalian cells: effects of mitotic inhibitors on cell cycle progression. *Genes*
565 *to cells : devoted to molecular & cellular mechanisms* **2**: 369-380.

566

567

Figure Legends

Fig. 1. High-throughput screening for drugs enhancing transfection efficiency.

(A) Schematic diagram of high-throughput screening system using luciferase reporter gene assay. A cell viability assay was performed using the RealTime-Glo™ MT Cell Viability Assay system. (B) MEF cells were treated overnight with 10 μ M of each compound from the Osaka University compound library. DMSO was used for negative controls. Luciferase activity and cell viability were measured, and the results are plotted. Red broken lines represent the mean + 4 \times SD of all negative control assay points.

Fig. 2. Second screening of compounds selected in high-throughput screening.

(A) MEF cells were treated for 16 h with 1 μ M each of the top 87 compounds identified in the primary screen. DMSO was used for negative controls. The relative fold change in the luciferase activity of each compound is plotted. The activity of DMSO-treated cells is set as 1. The second and third columns are colchicine and vinblastine as indicated. (B) List of top 10 potential compounds for enhancement of transfection efficiency. (C) MEF cells were treated with the indicated concentrations of colchicine (left graph) or vinblastine (right graph). The cells were transfected with the pCMV-Luc plasmid and incubated for 24 h, after which reporter gene assays were performed. Luciferase activity was normalized to cell viability. Black thick bars and thin lines indicate the mean and SD, respectively, of at least three independent experimental results. (D) MEF cells (a, d), 250 nM colchicine-treated MEF cells (b, e), and 50 nM

vinblastine-treated MEF cells (c, f) were examined using fluorescence microscopy 24 h after transfection of a GFP-expressing plasmid (upper panels; GFP); the lower panels represent the corresponding bright-field (BF) images of the upper panels. Scale bar = 250 μ m.

Fig. 3. Colchicine and vinblastine treated MEF cells do not enhance transfection efficiency in the absence of p62.

(A) p62KO-MEF cells were treated for 16 h with 1 μ M each of the top 87 compounds identified in the primary screen. DMSO was used for negative controls. The relative fold change in the luciferase activity of each compound is plotted. The activity of DMSO-treated cells is set as 1. The right two columns are reproduced from Fig. 2A for comparison. (B, C) p62KO-MEF cells were treated with the indicated concentrations of (B) colchicine or (C) vinblastine. These stable cell lines were incubated for 43 h, after which reporter gene assays were performed. Luciferase activity was normalized to cell viability. Each value is indicated as the mean \pm SD of at least three independent experimental results.

Fig 4. Colchicine and vinblastine treated MEF cells affect the timing of ubiquitination.

(A) Schematic diagram of experimental system using beads incorporated into cells to monitor behavior of transfected materials. (B, C) Time-lapse images of pHrodo and

GFP-Ub fluorescence around a single pHrodo bead in MEF cells. Images were obtained every minute for approximately 60 min. The panels show representative images of pHrodo and GFP-Ub fluorescence in (B) GFP-Ub MEF cells treated with DMSO as a control and (C) GFP-Ub MEF cells treated with 500 nM colchicine. Scale bar = 2 μ m. (D) Statistical analysis was performed for the timing of GFP-signal accumulation around the beads after the loss of pHrodo signals in the GFP-Ub MEF cells. The results are plotted as follows: mock control treated with DMSO (lane 1), 100 nM colchicine-treated MEF cells (lane 2), 500 nM colchicine-treated MEF cells (lane 3), and 100 nM vinblastine-treated MEF cells (lane 4). The median values were 4 min for GFP-Ub (n = 24 beads), 6 min for 100 nM colchicine (n = 28 beads), 6 min for 500 nM colchicine (n = 22 beads), and 6 min for 100 nM vinblastine (n = 31 beads). Three independent experiments were performed for each lane and the total bead number is indicated as n . Statistical differences (p < 0.0001) were determined using the Kruskal–Wallis test. Error bars indicate 95% confidence intervals.

Fig. 5. Colchicine and vinblastine treated MEF cells decrease the level of phosphorylated p62 at S405.

Western blot analysis was performed for total p62 and S405-phosphorylated p62 in MEF cells under the indicated conditions. GAPDH was used as a loading control.

Fig. 1

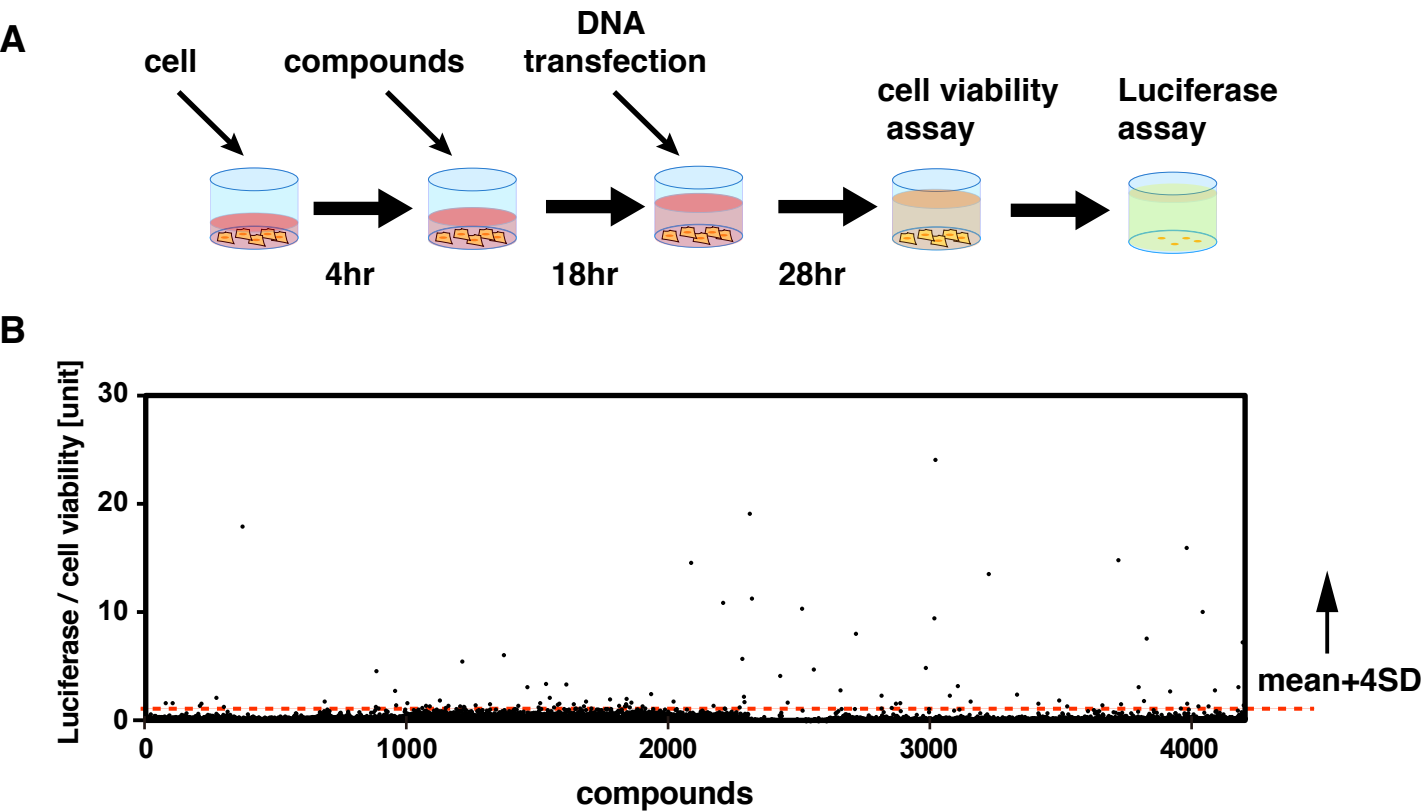


Fig. 2

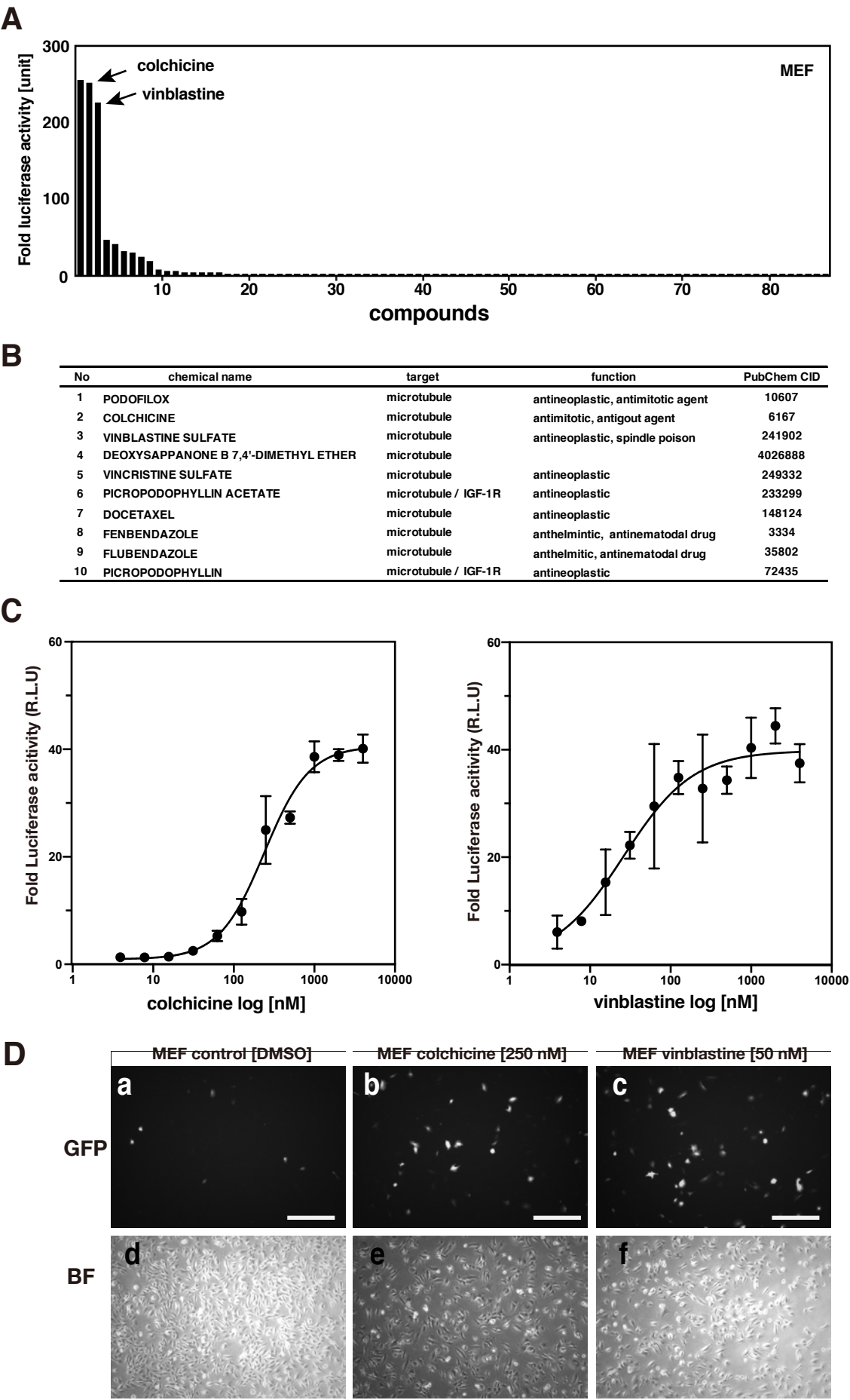


Fig. 3

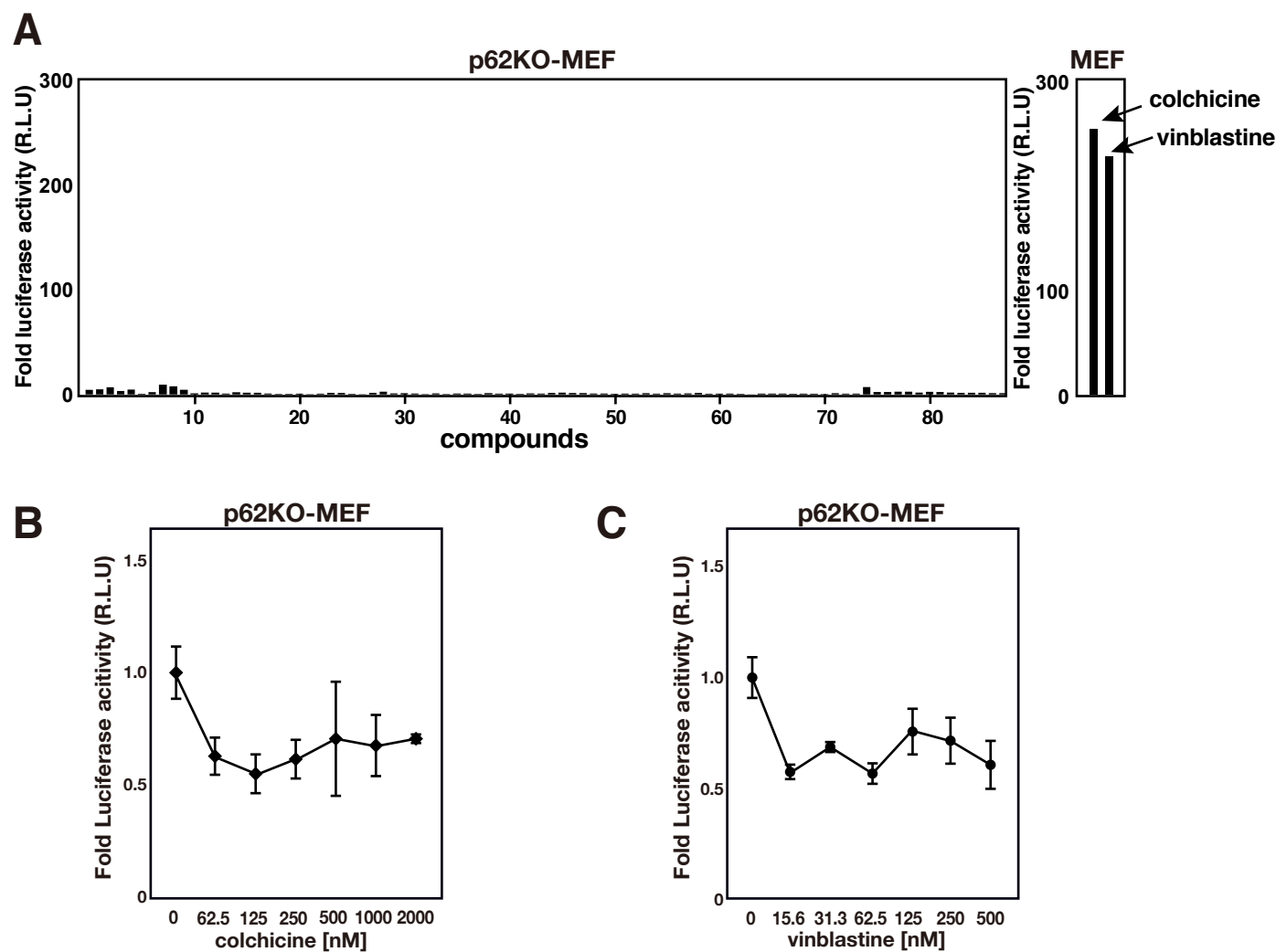
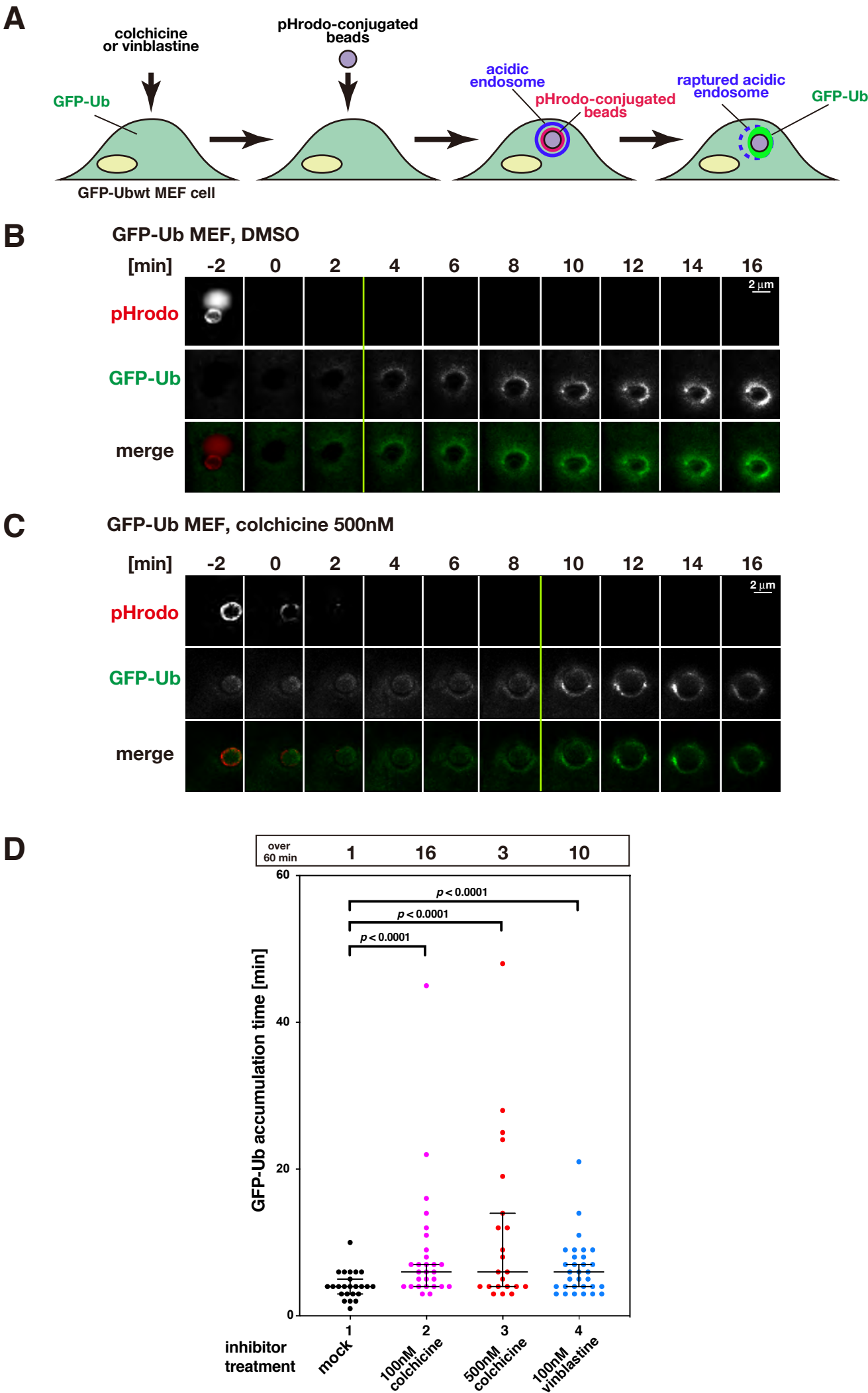


Fig. 4

bioRxiv preprint doi: <https://doi.org/10.1101/2021.05.13.443985>; this version posted May 13, 2021. The copyright holder for this preprint (which was not certified by peer review) is the author/funder, who has granted bioRxiv a license to display the preprint in perpetuity. It is made available under aCC-BY-NC-ND 4.0 International license.



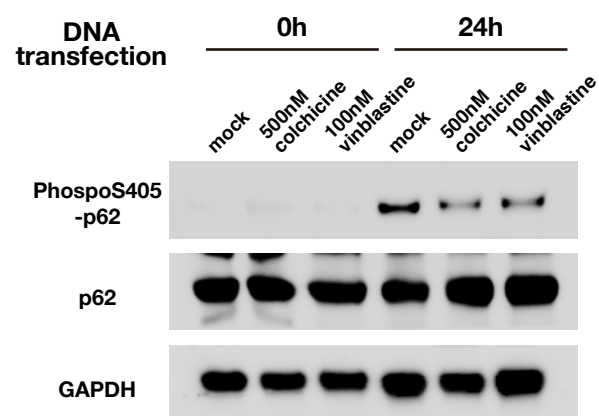
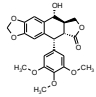
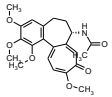
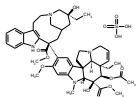
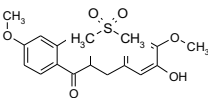
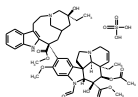
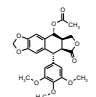
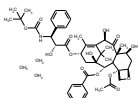
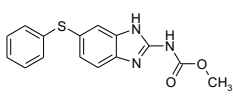
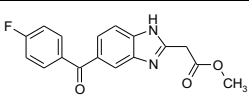
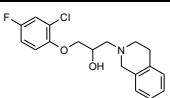
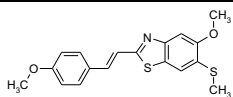
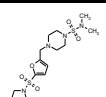
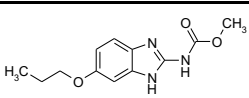
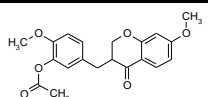
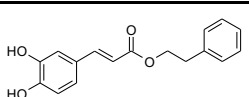
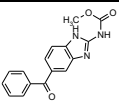
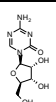
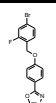
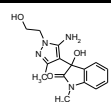
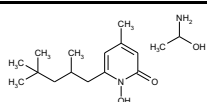
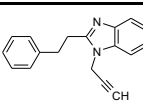
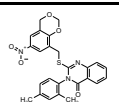
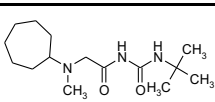
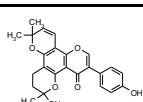
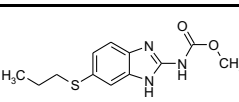
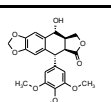
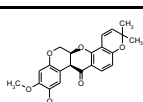
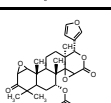
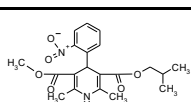
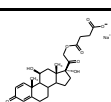
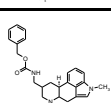
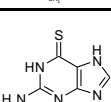
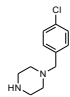
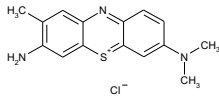
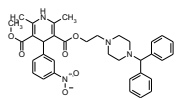
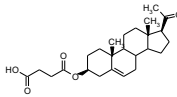
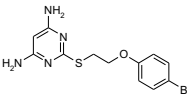
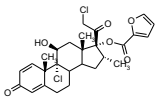
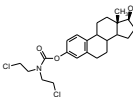
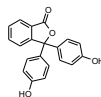
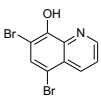
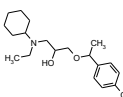
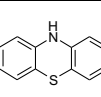
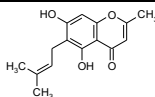
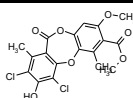
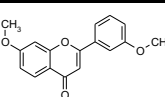
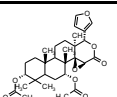
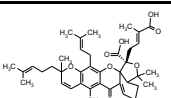
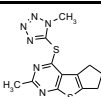
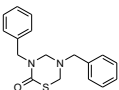
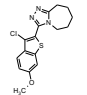
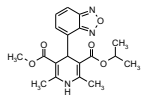
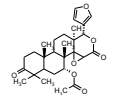
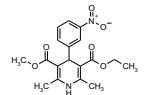
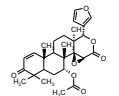
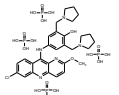
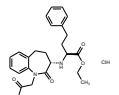
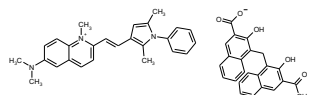
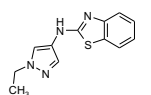
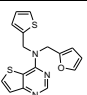
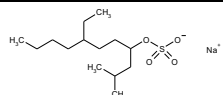
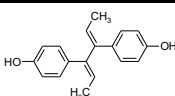
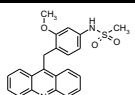
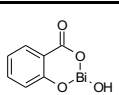
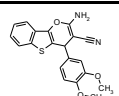
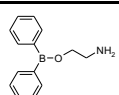


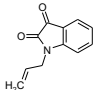
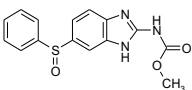
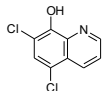
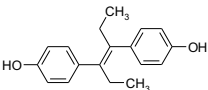
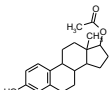
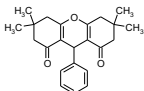
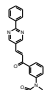
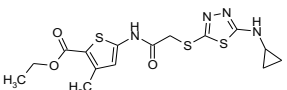
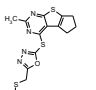
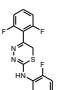
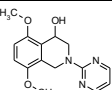
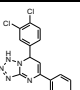
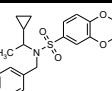
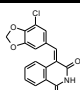
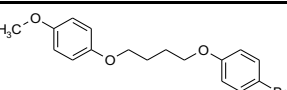
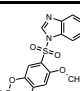
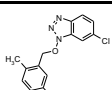
Table S1. Identification of 87 potential compounds for enhancement of transfection efficiency.

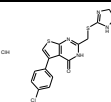
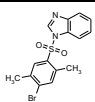
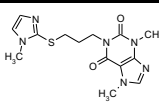
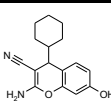
Rank	Structure	Name	Formula	Fold activity in MEF	Fold activity in p62KO-MEF
1		PODOFILOX	C ₂₂ H ₂₂ O ₈	297.24	4.46
2		COLCHICINE	C ₂₂ H ₂₅ N O ₆	294.20	4.94
3		VINBLASTINE SULFATE	C ₄₆ H ₅₈ N ₄ O ₉ · H ₂ O ₄ S	263.07	6.90
4		DEOXSAPPANONE B 7,4'-DIMETHYL ETHER	C ₁₈ H ₁₈ O ₅	54.43	4.72
5		VINCRISTINE SULFATE	C ₄₆ H ₅₆ N ₄ O ₁₀ · H ₂ O ₄ S	46.77	0.66
6		PICROPODOPHYLLIN ACETATE	C ₂₄ H ₂₄ O ₉	35.46	2.19
7		DOCETAXEL	C ₄₃ H ₅₃ N O ₁₄ · 3 H ₂ O	33.78	9.43
8		FENBENDAZOLE	C ₁₅ H ₁₃ N ₃ O ₂ S	27.14	7.83
9		FLUBENDAZOLE	C ₁₇ H ₁₃ F N ₂ O ₃	21.35	4.53
10			C ₁₈ H ₁₉ Cl F N O ₂	8.77	1.09
11			C ₁₈ H ₁₇ N O ₂ S ₂	6.80	1.80
12			C ₁₅ H ₂₆ N ₄ O ₅ S ₂	6.19	1.70
13		OXIBENDAZOLE	C ₁₂ H ₁₅ N ₃ O ₃	4.64	0.85
14		DEOXSAPPANONE B 7,3'-DIMETHYL ETHER ACETATE	C ₂₀ H ₂₀ O ₆	4.50	2.07
15		PHENETHYL CAFFEATE (CAPE)	C ₁₇ H ₁₆ O ₄	4.44	1.63

16		MEBENDAZOLE	C16 H13 N3 O3	3.01	1.57
17		AZACITIDINE	C8 H12 N4 O5	2.92	0.93
18			C15 H10 Br F N2 O2	2.84	0.53
19			C15 H18 N4 O3	2.52	0.62
20		PIROCTONE OLAMINE	C14 H23 N O2 . C2 H7 N O	2.04	0.78
21			C18 H16 N2	1.96	0.38
22			C25 H21 N3 O5 S	1.91	0.76
23			C15 H29 N3 O2	1.82	1.52
24		ISOOSAJIN	C25 H24 O5	1.59	1.50
25		ALBENDAZOLE	C12 H15 N3 O2 S	1.50	0.62
26		PICROPODOPHYLLIN	C22 H22 O8	1.49	0.32
27		DEGUELIN(-)	C23 H22 O6	1.44	1.51
28		EPOXYGEDUNIN	C28 H34 O8	1.37	2.66
29		NISOLDIPINE	C20 H24 N2 O6	1.32	1.05
30		METHYLPREDNISOLONE SODIUM SUCCINATE	C26 H33 O8 . Na	1.30	1.24
31		METERGOLINE	C25 H29 N3 O2	1.29	0.93
32		THIOGUANINE	C5 H5 N5 S	1.28	0.45

33			C11 H15 Cl N2	1.26	1.02
34		TOLONIUM CHLORIDE	C15 H16 N3 S . Cl	1.24	0.49
35		MANIDIPINE HYDROCHLORIDE	C35 H38 N4 O6	1.22	0.90
36		PREGNENOLONE SUCCINATE	C25 H36 O5	1.20	0.85
37			C12 H13 Br N4 O S	1.15	0.56
38		MOMETASONE FUROATE	C27 H30 Cl2 O6	1.14	1.26
39		ESTRAMUSTINE	C23 H31 Cl2 N O3	1.08	0.79
40		PHENOLPHTHALEIN	C20 H14 O4	1.07	0.86
41		BROXYQUINOLINE	C9 H5 Br2 N O	1.07	0.63
42			C19 H30 Cl N O2	1.06	1.04
43		PHENOTHIAZINE	C12 H9 N S	1.05	0.86
44		PEUCENIN	C15 H16 O4	1.05	1.45
45		GANGALEOIDIN	C18 H14 Cl2 O7	1.04	1.71
46		7,3'-DIMETHOXYFLAVONE	C17 H14 O4	1.01	1.43
47		3-ACETYLGEDUNOL	C30 H40 O8	1.00	1.37
48		GARCINOLIC ACID	C38 H46 O9	0.99	0.88
49			C12 H12 N6 S2	0.97	0.94

50		SULBENTINE	C17 H18 N2 O S	0.92	0.63
51			C16 H16 Cl N3 O S	0.92	0.85
52		ISRADIPINE	C19 H21 N3 O5	0.90	0.80
53		DIHYDROGEDUNIN	C28 H36 O7	0.90	1.23
54		NITRENDIPINE	C18 H20 N2 O6	0.88	0.82
55		GEDUNIN	C28 H34 O7	0.87	1.23
56		PYRONARIDINE TETRAPHOSPHATE	C29 H32 Cl N5 O2 . 4 H3 O4 P	0.87	0.83
57		BENAZEPRIL HYDROCHLORIDE	C24 H28 N2 O5 . Cl H	0.86	1.06
58		PYRVINIUM PAMOATE	C26 H28 N3 . C23 H15 O6	0.85	1.46
59			C12 H12 N4 S	0.83	0.70
60			C16 H13 N3 O S2	0.82	0.80
61		SODIUM TETRADECYL SULFATE	C14 H29 O4 S . Na	0.81	0.83
62		DIENESTROL	C18 H18 O2	0.81	0.61
63		AMSACRINE	C22 H20 N2 O3 S	0.81	0.18
64		BISMUTH SUBSALICYLATE	C7 H5 Bi O4	0.78	0.84
65			C20 H16 N2 O3 S	0.78	0.86
66		AMINOETHOXYDIPHEN YLBORANE	C14 H16 B N O	0.76	0.88

67			C11 H9 N O2	0.75	0.69
68		OXFENDAZOLE	C15 H13 N3 O3 S	0.73	0.80
69		CHLOROXINE	C9 H5 Cl2 N O	0.71	0.72
70		DIETHYLSTILBESTROL	C18 H20 O2	0.66	0.45
71		ESTRADIOL ACETATE	C20 H26 O3	0.60	1.21
72			C23 H26 O3	0.55	0.81
73			C22 H17 N3 O3	0.44	0.86
74			C15 H18 N4 O3 S3	0.41	7.11
75			C14 H14 N4 O S3	0.07	2.33
76			C15 H10 F3 N3 S	0.07	2.35
77			C15 H17 N3 O3	0.07	2.67
78			C16 H10 Br Cl2 N5	0.06	2.62
79			C20 H23 N O4 S	0.06	1.80
80			C17 H10 Cl N O4	0.06	2.52
81			C17 H19 Br O3	0.06	2.36
82			C15 H13 Cl N2 O4 S	0.05	1.75
83			C15 H14 Cl N3 O	0.04	1.52

84			C16 H13 Cl N4 O S2 . Cl H	0.04	1.59
85			C15 H13 Br N2 O2 S	0.03	1.58
86			C14 H18 N6 O2 S	0.03	1.26
87			C16 H18 N2 O2	0.03	1.27

Comparison of 87 compounds derived from the Osaka University compound library, showing their chemical structure, name, formula, and activity in 1 μ M of a 96-well luciferase assay in MEF cells and p62KO-MEF cells.

Fig. S1

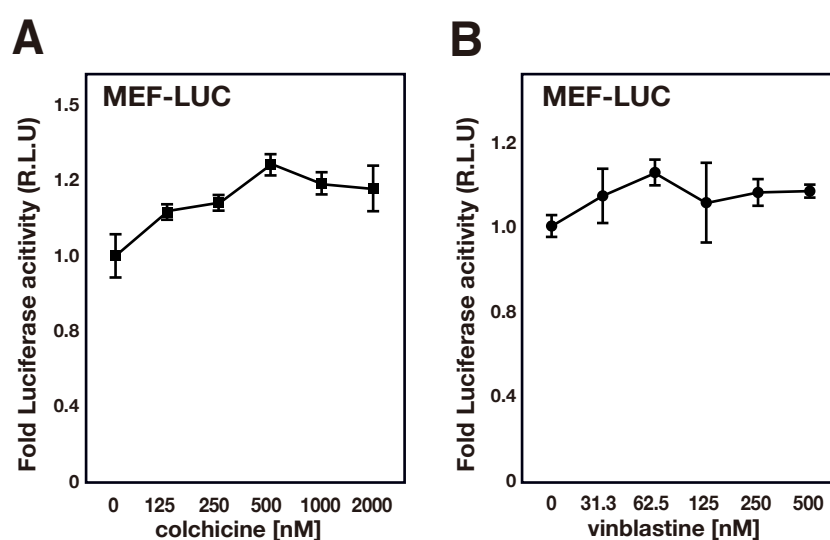


Fig. S1. Colchicine and vinblastine treatments do not affect the promoter activity of the luciferase gene.

(A, B) MEF cells stably expressing luciferase (MEF-LUC) were treated with the indicated concentrations of (A) colchicine or (B) vinblastine. After incubation for 43 h, the luciferase activity of the cells was measured and normalized to cell viability. Each value is indicated as the mean \pm SD of at least three independent experimental results.